Available online at www.sciencedirect.com
SCIENCE DIRECT®
Developmental Brain Research 141 (2003) 117–128
DEVELOPMENTAL BRAIN RESEARCH
www.elsevier.com/locate/devbrainres

Research report

Changes in cell cycle parameters and cell number in the rat midbrain during organogenesis

Thomas A. Lewandowski[a,b], Rafael A. Ponce[a,c], Jay S. Charleston[d], Sungwoo Hong[a], Elaine M. Faustman[a,*]

[a]Department of Environmental Health, University of Washington, Seattle, WA 98105, USA
[b]Gradient Corporation, Mercer Island, WA 98040, USA
[c]Zymogenetics Inc., Seattle, WA 98102, USA
[d]ICOS Corporation, Bothell, WA 98021, USA

Accepted 8 January 2003

Abstract

We employed 5-bromo-2′-deoxyuridine (BrdU) labeling to identify in vivo changes in the cell cycle patterns of the rat midbrain during the major period of midbrain organogenesis, gestational days (gd) 11 to 16. We also used quantitative stereology to determine changes in absolute cell numbers during these gestational time points. Between gd 12 and 16, the length of S-phase did not change significantly while the fraction of cycling cells decreased from 73 to 11%. The average cell cycle length was determined to be 15 h on gd 12 and 17 h on gd 16, the difference not being statistically significant. The cell number in the midbrain increased from 1.3E5 cells on gd 11 to 1.7E7 cells on gd 16. On gd 12 and gd 13, there was a significant negative correlation between litter position and midbrain cell number, the effect diminishing on later days of gestation. The combined use of quantitative stereology and flow cytometry to study brain development represents a novel application that allows for simultaneous evaluation of changes in cell proliferation kinetics and the resulting effect of those kinetic changes on embryonic midbrain development.

Theme: Development and regeneration

Topic: Genesis of neurons and glia

Keywords: Cell cycle; Proliferation; Midbrain; Development; Stereology

1. Introduction

Nervous system development in mammals follows a well-characterized pattern wherein neuronal production is followed by neuronal migration, synaptogenesis, selective cell loss, and myelination. As determined by ^{3}H-thymidine incorporation experiments, the various regions of the CNS develop and undergo maturation during different, discrete developmental periods, and the timing of neuronal precursor cell (neuroepithelial cell) proliferation varies by brain region, and within a region, by specific brain nuclei [1,36,52,67,68,72]. Such specificity in neuroepithelial proliferation facilitates the development of orderly connections between nerve foci in the nervous system [9] and the correct establishment of the cortical layers [13]. Impaired cell proliferation is suspected to underlie such neurodevelopmental diseases as spina bifida, holoprosencephaly, microcephaly, altered neurobehavior and mentation, and craniofacial abnormalities such as cleft lip and cleft palate [63,71,77].

Despite years of study, limited quantitative data exist regarding changes in mitotic activity in the normally developing brain. A number of studies using tritiated thymidine have identified proliferative periods in various brain regions during brain organogenesis. For example, Bayer and Altman used ^{3}H-thymidine studies to identify proliferative periods in various brain regions during normal brain organogenesis in the rat and other species

*Corresponding author. 4225 Roosevelt Way NE, Suite 100, Seattle, WA 98105, USA. Tel.: +1-206-685-2270; fax: +1-206-685-4696.
E-mail address: faustman@u.washington.edu (E.M. Faustman).

0165-3806/03/$ – see front matter
doi:10.1016/S0165-3806(03)00004-X

[6,7,10,11]. Rodier [62] summarized these primarily qualitative data to depict proliferative windows for various regions in whole brain development. Although these studies indicate the relative level of proliferation on different days of gestation, they do not provide data on actual cell cycle kinetics such as the cell cycle length, cell cycle phase transition durations, or changes in the fraction of proliferating cells. A limited amount of quantitative cell cycle kinetic data have been collected in the context of toxicology, where the effects of various teratogenic agents on cell proliferation were studied, but these typically involved evaluation at a single point in gestation (e.g., Refs. [24,31,64]). The work of Miller and colleagues [44–48] has yielded quantitative cell cycle kinetic parameters on cell proliferation in the rat cerebral cortex but this appears to be the only region of the developing rat brain studied in this manner.

In our work we used the technique of in vivo 5-bromo-2′-deoxyuridine (BrdU) labeling to identify normal changes in the cell cycle patterns of the rat midbrain during the major period of midbrain organogenesis, gestational days (gd) 11 to 16. BrdU, a thymidine analog, is incorporated into DNA during cell replication. Flow cytometric analyses of BrdU-labeled cells allows analysis of cell cycle phase (G_0/G_1, S, and G_2/M) by DNA content across one axis, and BrdU content, indicating active cell proliferation, across the other [28,30]. This technique has been used extensively to investigate the growth potential of tumors [12,29,38,74] and to investigate the cell cycle effects of several teratogens [25,35,45–48,53,59]. Pulse labeling, in which a single BrdU injection is given followed by analysis a short time afterwards, can be used with anti-BrdU antibody detection to estimate the amount of time cells are in the S-phase of the cell cycle [12]. For most cell populations, longer term labeling of DNA with BrdU is also required to determine the total fraction of cycling cells. Gathering data at both short and long periods allows for determination of several parameters of the cell cycle including the S-phase duration, the overall cell cycle time, and the total fraction of cells cycling [44,54].

To complement and confirm our cell cycle data, we used the cell counting methods of quantitative stereology [23,58] to determine absolute cell numbers over the studied gestational time points. Recent developments in stereology, based on the optical dissector and fractionation methods, have revolutionized the ability to perform unbiased cell counts in the central nervous system [34,42]. These stereology tools are increasingly being recognized as the appropriate method for determining cell number in the CNS [66]. These tools have been used to document neuron number in adult rodent models (e.g., Refs. [15,55,60,76]), in non-human primates (e.g., Refs. [21,22]) and humans [56,75]. As is the case for cell cycle kinetics, there is a dearth of data on changes in cell number in different brain regions during development. Data that have been collected typically involve limited time points and focus on specific nuclei [43,50,51] or grossly defined areas such as the cerebrum [33]. The use of quantitative stereology with BrdU-based flow cytometry to study brain development therefore represents a novel application that should significantly contribute to our understanding of the process of brain development.

2. Materials and methods

2.1. Animals

Time-mated female Sprague–Dawley rats were obtained from Charles River Laboratories (Hollister, CA, USA). The morning after mating was designated gd 0. Animals were shipped from the breeding facility to the University of Washington Health Sciences Complex on gd 6. Animals were kept on a 12-h light/dark cycle, fed with standard rat chow, and watered ad libitum. Animal care and treatment followed a university-approved animal use protocol developed in accordance with NIH guidelines.

2.2. Cell cycle kinetics studies

2.2.1. Treatment

Rats were dosed with BrdU on different gestational days to evaluate how cell cycle patterns change during the course of gestation. Short term (1.5 h) exposures to determine the S-phase length were carried out on gds 11, 12, 13, 14 and 16. These corresponded to Witschi stages 18, 21, 27, 29 and 32, respectively. Animals received a single intraperitoneal (i.p.) injection of BrdU (18 mg/ml dissolved in PBS, pH 7.7, total dose 25 mg/kg) and were sacrificed 1.5 h later. Preliminary work indicated that it required approximately 15 to 20 min for injected BrdU to reach the embryo in sufficient concentrations to cause detectable BrdU labeling of DNA. After sacrifice, tissues were collected and processed as described below. Long-term cumulative BrdU exposures to determine the total cell cycle length and fraction of cells involved in cycling were carried out on gd 12 and gd 16. These animals received injections of BrdU starting at 8 a.m. and continuing at 5 h intervals with animals sacrificed at various times to determine the change in the fraction of BrdU-labeled cells. Initial work indicated that an interval of 5 h between BrdU injections was sufficient to label all cycling cells (i.e., no cycling cells would pass completely through S-phase without being labeled in 5 h).

2.2.2. Tissue collection

At the appropriate time interval after BrdU injection, animals were killed using CO_2. To evaluate the potential effects of BrdU toxicity on cell cycle progression, embryos were also obtained on gd 12 from four dams not treated with BrdU. The uteri were removed and placed on ice and

maintained cold while embryos were dissected out of the uterine tissues. Dissection on ice was observed to halt BrdU incorporation in embryonic tissues and allowed for precise control of the time of BrdU exposure. After the embryos were obtained from the uteri, the developmental stage was confirmed by measuring crown rump length, counting somites, and evaluating overall morphology and comparing these to a standard reference [2]. The embryonic midbrains were then sectioned from the main part of the embryo. The midbrain was identified as indicated in Fig. 1. This area included the developing region of the thalamus. The inclusion of the thalamus as part of the midbrain structure for the purposes of counting was done to enable use of the unambiguous boundary formed by the prominent fissure separating the thalamus from the cerebral cortex. The midbrains obtained from each litter were pooled and disaggregated using 0.25% trypsin/2.5% collagenase and trituration. The cell suspensions were then washed with PBS/5% Normal Goat Serum (NGS) and cells were fixed in cold 70% ethanol. All work was conducted using dark room lights to minimize BrdU photoactivation [26,39,61].

2.2.3. Cell staining

Cells were centrifuged (10 min, 700 rpm for all spins) in 70% ethanol and then resuspended in 1 ml PBS/5% NGS. Cells were allowed to rehydrate overnight as this was found to provide better antibody access to DNA. After the overnight rehydration, cells were centrifuged and resuspended in 150 μl of PBS/NGS and 450 μl of membrane shredding solution (100 ml CMF-PBS, 500 μl NP-40, 20 mg EDTA). Samples were placed on ice and vortexed vigorously every 3 min for 20 min. Samples were then acidified with 800 μl of 4 N HCl and agitated for 45 min at room temperature to denature the double stranded DNA and allow antibody access. Cells were then washed twice with 3 ml 1 M Tris (pH 8.5) and counted using a hemocytometer. The samples were then completely decanted and resuspended with a FITC-conjugated anti-BrdU antibody (Pharmingen, San Diego, CA, USA) at a ratio of 150 μl antibody to 1E6 cells. The antibody was previously diluted to 1:20 with PBS/NGS/0.5% Tween 20. After 1 h of incubation, samples were washed once with PBS/NGS and resuspended in PBS for flow analysis. Immediately prior to flow analysis, the DNA stain propidium iodide (PI) was added to achieve a final PI concentration of 5 μg/ml in the sample.

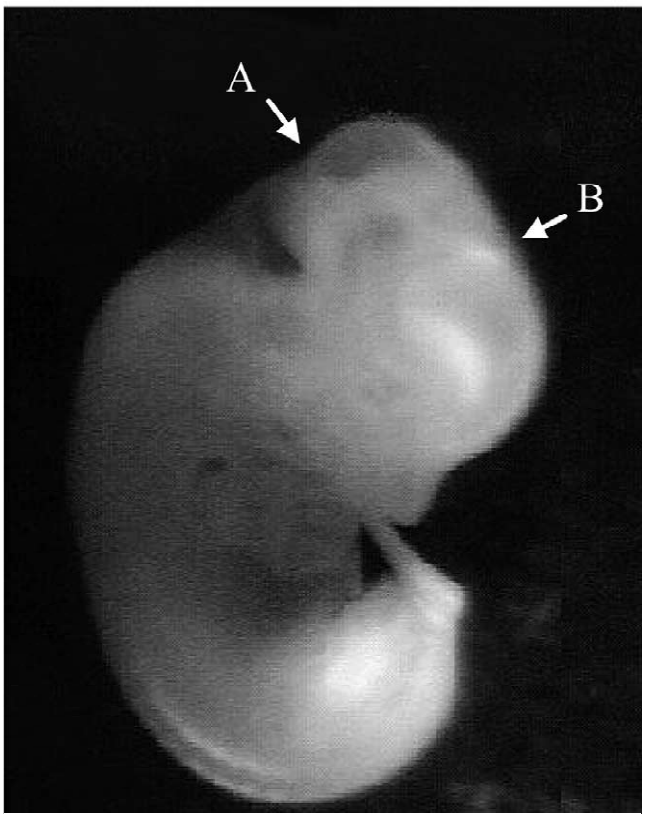

Fig. 1. Rat embryo (gd 14) indicating the region being studied. Arrow A indicates the cerebellomesencephalic flexure while arrow B indicates a similar flexure, associated with the posterior commissure [2,57]. These markers are discernable between gd 11 and gd 16.

2.2.4. Flow cytometry

Flow cytometry was used to determine the fraction of cells positively labeled with BrdU and the cell cycle profile (i.e., %G1, %G2 and %S). Dual parameter flow cytometry utilized a Coulter EPICS Elite equipped with a coherent Innova 90 air-cooled argon laser. Excitation occurred at 488 nm for both FITC and PI. Fluorescence measurements were obtained from approximately 20,000 cells. Data was analyzed using the software package Mplus (Phoenix Flow Systems, San Diego, CA, USA).

2.2.5. Cell cycle kinetic parameter estimation

The S-phase length (T_s) was determined from the pulse labeling study by the shift in mean PI fluorescence of the BrdU-labeled cells after 1.5 h of BrdU exposure using the method of Begg et al. [12] as modified by Terry et al. [73]. The total cell cycle duration (T_c) was determined graphically as the time required for all actively cycling cells to be labeled plus the previously calculated S-phase duration [54].

As an alternative approach, the cell cycle time was estimated using analytical methods developed by Bertuzzi et al. [14]. In this approach, the T_c can be estimated analytically with rearrangement of his Eqs. (2) and (5) to yield

$$T_c = \frac{\lambda \times T_s}{LI} \times \frac{\ln(1 + GF)}{\ln 2}$$

where T_s can be estimated using the relative movement method (described above), LI can be estimated as the fraction of cells labeled with a single pulse of BrdU, and the growth fraction (GF) can be estimated from continuous BrdU labeling.

2.2.6. BrdU toxicity

To evaluate potential BrdU toxicity, the cell cycle phase distribution (i.e., the percentage of the midbrain cells in each phase of the cell cycle as determined by PI staining and the Mplus software) in BrdU-treated animals was compared to the distribution in untreated controls. Data were evaluated for statistical significance using *t*-tests or ANOVAs and a significance criterion of 0.05.

2.3. Cell counting

2.3.1. Embryo isolation

Using a separate set of dams (i.e., without BrdU treatment), embryos were obtained on gds 11, 12, 13, 14 and 16 using the procedures described above. On gd 11, one litter was evaluated whereas two litters were evaluated on each of the other days. The location of each embryo on the uterine horn was preserved so that uterine position effects on cell number could be determined. After collection, each embryo was assigned a specific code number so that counting was performed with the observer blind to uterine position. Four individual embryos were counted per litter.

2.3.2. Tissue preparation

A detailed description of the technical details of the stereology procedure is available in Charleston [23]. Following fixation by whole body immersion in 4% paraformaldehyde (carried in 0.1 N dibasic sodium phosphate buffer, pH 7.2), whole bodies or heads of embryos (depending on age/size) were specifically positioned by embedment in 3% agar matrix to facilitate handling during subsequent tissue processing and increase histology efficiency by allowing entire sets of embryos to be processed together as a single tissue set. The agar blocks (containing the tissue) were dehydrated in a graded EtOH series and embedded in glycol methacrylate (Historesin, Cambridge Instruments, Deerfield, IL, USA). Blocks were exhaustively sectioned in the sagittal plane at a thickness of 20 or 30 μm on a JB-4 microtome (Sorvall) using glass knives and all sections were collected in the order generated. Sections were stained with Giemsa (stock solution, J.T. Baker, Phillipsburg, NJ, USA) using the procedure of Iñiguez et al. [37] following the suggestions of Brændgaard et al. [18,19].

2.3.3. Stereology

Estimates of the number of neurons in the developing rat midbrain were determined by use of the Optical Volume Fractionator (OVF) procedure of Bolender and Charleston as previously described [16,23]. The OVF procedure employs a design-based, systematic random, multilevel sampling protocol. Estimates of the cell number, *N*(cells, structure), are calculated as the product of the numerical density of the cell, N_v, and the structure volume, *V*(structure):

$$N(\text{cells, structure}) = N_v(\text{cell/volume}) \times V(\text{structure})$$

The structure volume, *V*(structure), was estimated by summing the volumes of a systematic subsample of all of the sections (obtained from exhaustively sectioning the brains) and then multiplying the subsample volume by the ratio of the total number of sections to the number of sections included in the subsample (e.g., 10 for a 1 in 10 sampling frequency). The volume of the sampled sections was estimated as the sum of the area of the sections multiplied by the average thickness of the sections.

The numerical density (N_v) of cells was determined with the optical disector. The area of the disector was set by an unbiased counting frame and its height measured by a length recording gauge attached to the microscope stage. Nuclei were counted when they came into focus as the focal plane was moved through a volume of the relatively thick (20 to 30 μm) section following the unbiased counting rules for the optical disector, and established cell recognition rules. We assumed that each cell type contains only one nucleus, hence nuclei counts equaled cell number in the disector volume.

Table 1 illustrates the results from the analysis of a typical individual embryonic midbrain. The table also describes the method used to estimate the sampling error (the observed coefficient of error, OCE). The estimator of the OCE is modeled after West and Gundersen [75], and provided the means to ascertain that the contribution of the sampling error for each individual contributed negligibly towards the observed group variance. The typical sampling hierarchy scheme differed depending upon the gestational day examined. The goal was to observe between 100 and 300 neuroepithelial cells per individual encountered across a set of systematic randomly selected sections and systematical randomly placed disector counting frames [23]. The smaller gd 11 brains were sampled by placing disectors on every second section from the exhaustive set of sections generated. In contrast, for the much larger gd 14 brains, it was determined that counting could be performed on every 12th section in the set of sections. Likewise, the spacing of the disector counting frame spacing was also increased as the developing brain increased in size. These adjustment in the sampling details were done to maintain the goal of counting only 100 to 300 neuroepithelial cells per individual, and thereby avoid excess work which would not appreciably improve number estimates. The boundaries of the fetal midbrain were determined by use of a developmental rat atlas [2]. Areas considered for cell enumeration are indicated in Fig. 1. As indicated previously, this area included the developing region of the thalamus, thus enabling use of the unambiguous boundary formed by the prominent fissure separating the thalamus from the cerebral cortex. Otherwise, determination of the boundary between the midbrain and thalamus would have required the use of arbitrary boundaries resulting in an equally arbitrary estimate of the

Table 1
Example calculations used in cell counting (representative data from a gd 14 animal)

Section (i)	P_i	$P_i \times P_i$	$P_i \times P_{i+1}$	$P_i \times P_{i+2}$	Q_i^-	F_i	$Q_i^- \times F_i$	$(F_i \times Q_{i+1}^- + F_{i+1} \times Q_i^-)/2$	$(F_i \times Q_{i+2}^- + F_{i+2} \times Q_i^-)/2$	N_i
1	2	4	26	18	10	2	20	116	93	10
2	13	169	117	182	51	13	663	541.5	825	51
3	9	81	126	45	48	9	432	660	223.5	48
4	14	196	70	0	72	14	1008	341	0	72
5	5	25	0	0	23	5	115	0	0	23
Sum	43	475	339	245	204	43	2238	1658.5	1141.5	
		A	B	C			D	E	G	
CE	0.119				0.101					0.101

P_i indicates the point counts per section (i) over the midbrain, and was used to estimate surface area of the sections containing midbrain because each point was associated with a known area. The total volume of the midbrain (V) can be calculated from the fraction of the total volume the sections represent, 1/12th, and the average section thickness, 29.7 μm. Q_i^- indicates the neuroepithelial counts in the disectors placed on each section. The number of disectors placed on each section (F_i) also equals the number of points (by design). N_i equals the number of cells counted per section i. Knowing the area of the disector counting frame and the height of each disector, the volume of the disectors is known, allowing calculation of numerical density (number per volume, N_v). Combining N_v with V yields a dimensionless estimate of the total cell number. In this example, the total number of neuroepithelial cells was calculated as 4.22E6. Formula (1) is used to calculate the observed coefficient of error (OCE) for each quantity. Formula (2) is an intermediate calculation of the covariance between P_i and Q_i^-. Formula (3) estimates the OCE after combining the results from formulas (1) and (2). Note that $F_i = P_i$, and $Q^- = N_i$. Adopted from West and Gundersen [75].

$$CE(\sum P_i) = \frac{\sqrt{(3A + C - 4B)/12}}{\sum P_i} = 0.119 \quad (1)$$

$$\mathrm{Cov}(\sum Q_i^-, \sum F_i) = \frac{(3D + G - 4D)}{12} = 101.8 \quad (2)$$

$$OCE(\sum Q_i / \sum F_i) = \sqrt{(CE^2(\sum Q_i^-) + CE^2(\sum F_i) - (2\,\mathrm{Cov}(\sum Q_i^-, \sum F_i)/\sum Q_i^- \times \sum F_i)} = 0.035. \quad (3)$$

total number of neuroepithelial cells. This area of interest was identified by extending a line between the base of the cerebellar sulcus and the base of the thalamus, thereby transecting the ventricular space. This approach was consistent with that used for collection of cells for the cell cycle kinetics evaluation. Correspondence between the atlas drawings and photographs with the histology sections was very good.

To adjust for inter-litter differences on those days where more than one litter was counted (gds 12, 13, 14 and 16), the cell number for each embryo was compared to the mean cell number for the individual litter. Inter-litter differences may be attributable to slight differences in mating time and would represent a potential confounder in our dataset. Linear regression analyses were performed for each gestational day to determine if litter position had a significant effect on midbrain cell number. To evaluate any interaction between litter position and gestational age, log-transformed data were analyzed using linear multiple regression with uterine position, gestational age and an interaction term as independent variables.

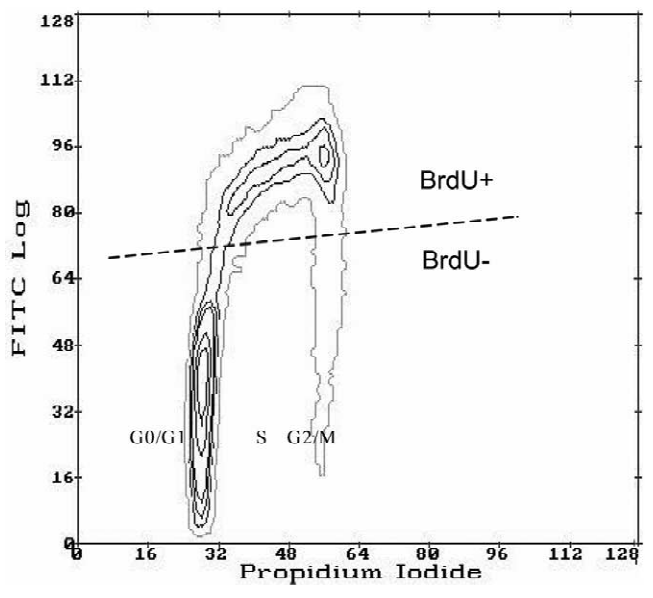

Fig. 2. Representative flow cytogram showing anti-bromodeoxyuridine (BrdU) antibody staining of midbrain cells (obtained on gestational day (gd) 12). Those cells shown above the dotted line are fluorescein isothiocyanate (FITC) (i.e., BrdU)-positive, having incorporated BrdU during the most recent S-phase of the cell cycle. Those below the dotted line are FITC negative, the baseline signal being due to cellular autofluorescence. Note that there are no FITC-negative S-phase cells, suggesting that embryonic BrdU levels were sufficient to label all proliferating cells.

3. Results

3.1. Cell cycle kinetics studies

A BrdU dose of 25 mg/kg was found to be sufficient for clear resolution of BrdU-negative and -positive cells using

Table 2
Results for bromodeoxyuridine (BrdU) pulse labeling studies

Gestational day	T_s (h)	(S.D.)	Pct BrdU positive	(S.D.)
11	7.5	0.9	51	1.8
12	8.2	1.5	32.6	2.2
13	8.6	1.3	27.5	5.8
14	7.5	1.0	11.2	1.5
16	11.3	3.4	6.6	1.4

Maternal animals were injected with 25 mg/kg BrdU and embryos were evaluated 1.5 h later. The percent of BrdU-positive cells was found to change significantly at the gestational times evaluated (ANOVA, $P<0.01$). Differences in S-phase length (T_s) were not statistically significant. Each data point represents data for five litters.

an anti-BrdU antibody (Fig. 2). Attempts were made to perform cell cycle analysis using the Hoechst quenching technique, in which BrdU incorporation is quantified by the BrdU-induced quenching of the fluorochrome Hoechst 33258. However, doses of 25 mg/kg BrdU were insufficient to clearly distinguish labeled and unlabeled cells by Hoechst quenching.

3.1.1. Pulse labeling studies

The S-phase length (T_s) for the gestational period studied is indicated in Table 2. Between gd 11 and 16, the length of S-phase did not change significantly. There was an indication of an increasing S-phase length on gd 16, but increased inter-litter variability at this time point precluded this finding from being statistically significant.

The fraction of cells labeled with a single BrdU pulse is also indicated in Table 2. This fraction of labeled cells is a reasonable estimate of the instantaneous labeling index (LI). Unlike the S-phase length, this parameter changed significantly over the different days of gestation (ANOVA, $P<0.01$), from a maximum of 51% on gd 11 to a minimum of 7% on gd 16. Note that this data provides an estimate of the relative degree of proliferation on the different gestational days but does not indicate the total number of cycling cells that can only be determined by continuous labeling.

3.1.2. Continuous labeling studies

The relative fractions of BrdU-stained cells following long-term BrdU labeling are shown for gd 12 and gd 16 in Fig. 3. An exponential function (Pct $\mathrm{BrdU}^+ = x_1^*[1-\exp(x_2 \times \mathrm{time})]$) was fit to the data using a maximum likelihood optimization and used to determine the point at which the plateau in BrdU labeling (the GF) was obtained. The GF was considered reached when the function reached 95% of the asymptotic final value. The fraction of actively cycling cells (the growth fraction, GF) changed markedly, from 73% (±4%, S.D.) on gd 12 to 11% (±1%, S.D.) on gd 16. This finding parallels those observed with the pulse labeling study described above and indicates a significant proportion of the cells are exiting the actively proliferating population by gd 16.

3.1.3. Estimated cell cycle time

Using the fitted exponential function and the method of Nowakowski et al. [54], the time to reach the labeling plateau (i.e., $T_c - T_s$) was 7 h on gd 12 and 6 h on gd 16. When combined with the S-phase length determined from the single pulse labeling study, the average cell cycle length (T_c) was found to be 15 h on gd 12 and 17 h on gd 16 (Table 3). Because the S-phase length was not found to be statistically different between gd 12 and gd 16, the

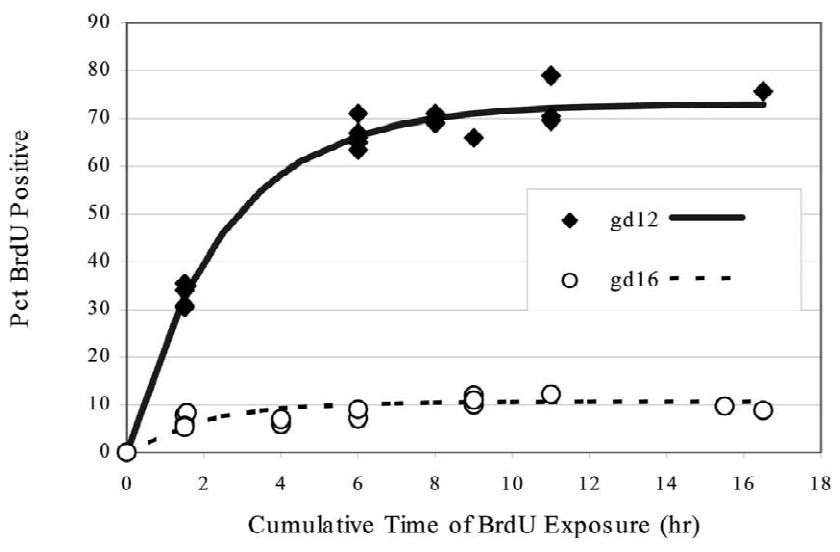

Fig. 3. Results for cumulative BrdU labeling at gd 12 and gd 16. Animals were given 25 mg/kg BrdU at 5 h intervals beginning at 8 a.m. on the relevant gestational day and then sequentially sacrificed at the times indicated. The fraction of BrdU-labeled cells in the midbrains was then determined using flow cytometry. The curves shown were fit using the maximum likelihood approach. On gd 12, the total fraction of cycling cells was found to be 73% (±4%, S.D.). The time required to reach this plateau ($T_c - T_s$) was approximately 7 h. On gd 16, the total fraction of cycling cells was observed to be 11% (±1%, S.D.). The time required to reach this plateau was approximately 6 h.

Table 3
Estimated vs. observed cell number in the developing rat midbrain

GD	N_0	GF	T_c (h)	Predicted cell number at the start of the next GD	Observed cell number (S.D.)
12	*3.60E+05*	*0.73*	*15*	1.7E+06	*3.6E+05 (1.2E+05)*
13	1.7E+06	*0.4*	*16*	4.6E+06	*1.6E+06 (0.3E+06)*
14	4.6E+06	*0.3*	*16*	1E+07	*3.9E+06 (0.4E+06)*
15	1E+07	*0.2*	*17*	2E+07	nd
16	2E+07	*0.11*	*17*		*1.7E+07 (0.2E+07)*

Predicted cell number after a period of exponential growth using derived cell cycle kinetic parameters. Values for growth fraction (GF) and cell cycle time (T_c) on gds 13–15 (in italics) were estimated so as to yield the observed number of cells on gd 16 (see text for details). Experimentally derived values for GF, T_c, and the observed number of cells by quantitative stereology are shown in italic text. The fifth column indicates the predicted cell number at the end of a given gestational day. This number becomes the model input for the next gestational day (column 2) and should be compared to the observed cell number shown in column 6. Cell number was not determined (nd) on gd 15.

difference in cell cycle length on these 2 days was also not statistically significant.

The cell cycle time (T_c) was also estimated analytically using the method of Bertuzzi et al. [14]. This method, originally developed to estimate cell cycle kinetic parameters in exponentially growing tumor cells, yielded results similar to those of Nowakowski et al. However, this method requires use of a somewhat arbitrary value, λ, which is selected based on estimates of the age distribution of the population and the phase transit times [14]. Bertuzzi et al. [14] recommend use of a value of $\lambda = 0.8$ when dealing with exponentially growing tumor cells. We assumed a comparable value of λ in our model, since cells were assumed to be growing exponentially, and there was no compelling reason to believe that the analytic model could not be applied to the developing embryonic nervous system. Using this method, the average cell cycle length (T_c) was found to be 15.7 h on gd 12 and 19.4 h on gd 16 (Table 3).

3.1.4. BrdU toxicity

The cell cycle distributions of BrdU-treated and control animals are shown in Fig. 4. There was no statistically significant difference between BrdU-treated and control animals (*t*-test, $P > 0.1$), thus indicating no significant effect of BrdU treatment on cell cycle progression.

3.2. Gestational changes in midbrain cell number

Histologic evaluation of Giemsa-stained midbrain sections demonstrated a preponderance of uniformly stained cells in a columnar arrangement localized to the ventricular walls, which is characteristic of neuroepithelial cells [49]. The Giemsa staining procedure characteristically stains the nuclei of neuronal cells a uniform pale blue, with the nucleolus appearing slightly darker. The cytoplasm of the neuroepithelial cell stains a deeper blue, and in adult neuronal cells embedded in glycol methacrylate, this staining pattern has been associated with Nissl [15,19]. The preponderance of cells encountered clearly possessed the morphology and staining characteristics of the neuronal cell type as described above, and were readily distinguished from other cell types (e.g., capillary endothelia, red blood cells) (Fig. 5). In the rat, the rapid development of the brain consists almost entirely of the growth of the neuroepithelial cells of the proliferative matrix between gd 11 and 14, with a gradual increase in differentiation into mature neurons adding to the volume of the brain paren-

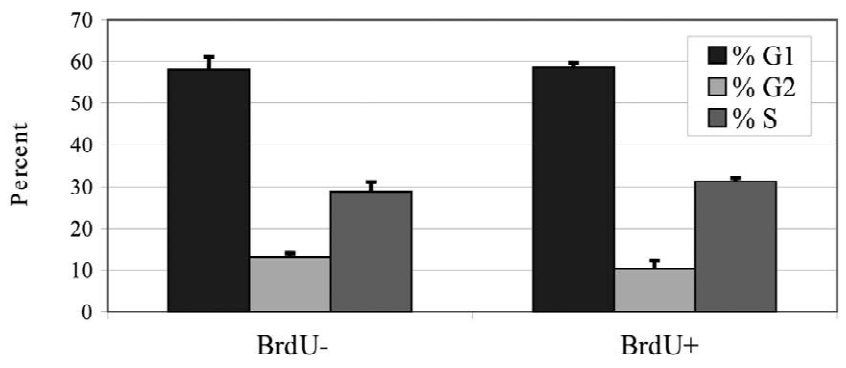

Fig. 4. Effect of BrdU treatment on cell cycle phase distribution. BrdU-treated animals received 25 mg/kg BrdU and were evaluated 6 h later. Animals were evaluated on gd 12. There was no statistically significant difference between BrdU-treated and control animals (*t*-test, $P > 0.1$).

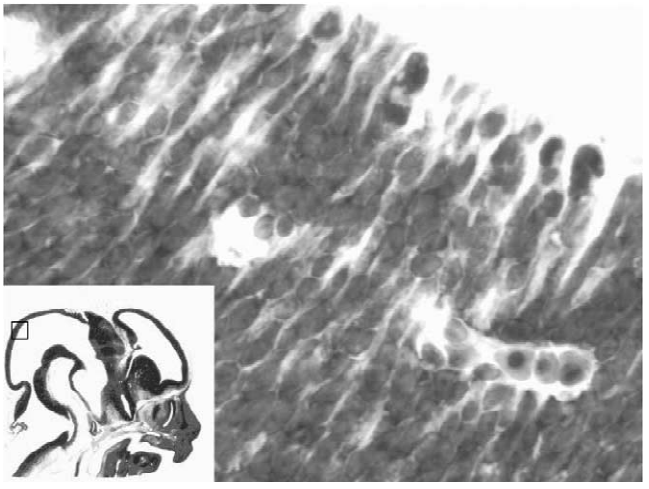

Fig. 5. Representative embryonic midbrain section used in stereology evaluations. Embryos were embedded in glycol methacrylate, sectioned and stained with Giemsa stain. Neuroepithelial cells (solid dark stain) were counted when they came into focus as the focal plane was moved through the relatively thick (20 to 30 μm) section. As indicated in the figure, nearly all of the cells encountered were of the neuroepithelial cell type. The region shown under 60× magnification is indicated in the 1× magnification image by the black square.

chyma accompanied by continued proliferation of neuroepithelial cells in the proliferative matrix between gds 15 and 18 [2,8].

3.2.1. Changes in midbrain neuroepithelial cell number over time

The change in the number of neuroepithelial cells, as estimated by quantitative stereology, from gd 11 to gd 16 is shown in Fig. 6. From a value of 1.3E5 cells (±3E4, S.D.) on gd 11 the midbrain reached a total of 1.7E7 cells (±1.7E6) on gd 16. The inter-embryonic variability appeared to decrease with advancing gestational age, with a coefficient of variation of 24% on gd 11 and a CV of 10% on gd 16. The estimation of the OCE associated with the individual number estimates indicates that the sampling scheme was more than sufficient to estimate mean cell number per time point.

The observed number of neuroepithelial cells in the embryonic rat midbrain can be compared against predicted cell number estimates using the experimentally derived cell cycle kinetic parameters and assuming exponential growth. For example, the following exponential growth model was used to estimate the number of cells in the gd 13 and 16 rat midbrain given cell cycle parameters estimated on gd 12 and 14, respectively:

$$N_{\text{Total}} = N_0 + GF \times N_0 \exp^{GR \times \Delta T}$$

where N_{Total} is the predicted number of cells over the time period (ΔT), given the starting number of cells (N_0), the growth fraction (GF), and the growth rate (GR, estimated as $1/T_c$). The predicted cell numbers using this model are compared against observed stereologic counts in Table 4. Because experimentally derived estimates of GF and T_c on gd 14 and 15 were not available, we assumed values for these parameters so as to yield the observed number of neuroepithelial cells on gd 16. Various other realistic assumptions about GF and T_c on gd 14 and 15, which are bounded by values observed on gd 12 and 16, also yield

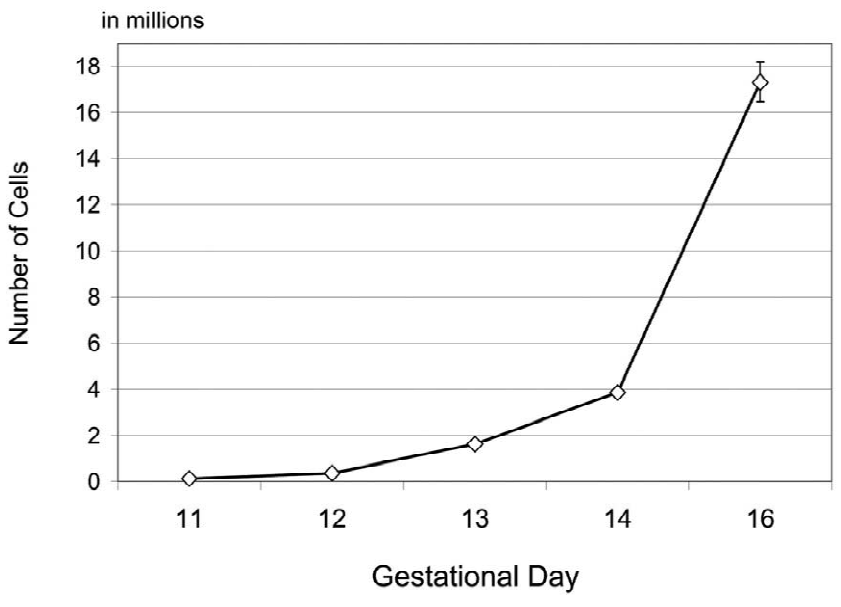

Fig. 6. Increase in total number of midbrain neuroepithelial cells with increasing length of gestation. Embryos were obtained from dams on the days indicated, fixed, embedded and then counted using the Optical Volume Fractionator (OVF) procedure. Error bars shown represent one standard deviation.

Table 4
Estimated cell cycle times based on experimental data

GD (days)	T_s (h)	LI (unitless)	GF (unitless)	Estimated T_c (h)	
				Bertuzzi	Nowakowski
12	8.2	0.33	0.73	15.7	15
16	11.3	0.07	0.11	19.4	17

Average cell cycle time of dividing cells as estimated using the analytical method of Bertuzzi et al. [14] compared to results obtained using the graphical method of Nowakowski et al. [54].
The labeling index (LI) was approximated by the percent BrdU positive indicated in Table 1.

estimated cell numbers on gd 16 similar to those obtained via stereology.

3.2.2. Positional effects

An evaluation of the cell count data suggests an effect of uterine position on midbrain cell number, at least on earlier gestational days (Table 5). A regression of percent change from the litter mean against litter position was used to determine if litter position had an effect on midbrain cell number. As shown in Table 5, there was a negative correlation between litter position and midbrain cell number, with embryos further from the center of the uterine horn having fewer midbrain cells. The effect was significant only on gd 12 and gd 13 ($P<0.10$) and there appeared to be an overall trend of decreasing importance of uterine position with advancing gestational age. A multiple regression analysis, accounting for interaction between gestational age and litter position, did not find a significant interaction between the two terms ($P>0.10$).

4. Discussion

In this paper we explored changes in cell cycling and cell number in the developing midbrain during a key period of organogenesis. Our cell cycling data for the rat midbrain appear to be generally in agreement with the data reported by Miller et al. [47] for the rat cerebral cortex. They observed that S-phase duration remained fairly stable throughout this period of gestation, at approximately 7–8 h, a value very similar to that reported here. They also observed that the fraction of cells cycling declined from approximately 90% on gd 13 to about 35% on gd 17. We similarly saw a decline from approximately 73% on gd 12 (equivalent to gd 13 in the Miller et al. study due to differences in time-mating terminology) to approximately 11% on gd 16. Given that the peak period of midbrain development in the rodent occurs about 1 day ahead of forebrain development [65], our slightly lower values appear to be reasonable. Miller and Kuhn [47] also observed that the overall cell cycle time increased from 12 h on gd 13 to 15 h on gd 17. Our estimates of the cell cycle time also increased, from 15 h on gd 12 to 17 h on gd 16, although these are largely due to changes in S-phase length which were not statistically significant. The slightly longer cell cycle times we observed in the midbrain relative to Miller's forebrain data may be due to methodological differences or may represent a true difference between the two brain regions, consistent with the earlier development of the midbrain.

Two methods were used to estimate the average cell cycle time for dividing neuroepithelial cells in the embryonic rat midbrain. The graphical method of Nowakowski et al. [54] assumed steady-state growth, wherein one of the two daughter cells produced following one round of the cell cycle did not re-enter the cell cycle. In contrast, the analytic method of Bertuzzi et al. [14] assumed exponential growth, wherein both daughter cells progressed through subsequent cell cycles. We demonstrate that the method of Nowakowski et al. yielded results comparable to those obtained by Bertuzzi et al. The method of Bertuzzi et al., originally developed to describe exponentially growing tumor cells, requires an assumption for the parameter λ for which there is no experimental basis in the developing rat CNS. Using a value of $\lambda = 0.8$, which works well for tumor cell kinetic parameter estimation, provides an average cell cycle time in the range estimated by the method of Nowakowski. Estimates of the T_c can vary widely within the theoretical range of λ (0.693 to 1.4), so small errors in this parameter can dramatically alter the estimated average cell cycle time.

The experimentally derived cell cycle kinetic parameters can be used in predictive models of neuroepithelial cell growth in the embryonic rat midbrain. As shown in Table 4, the predicted number of cells on gd 13 can be estimated from data available on gd 12 with no assumptions other than exponential growth. In addition, the number of cells in the gd 16 rat midbrain can be estimated from the cell number available on gd 12 and realistic estimates of the growth fraction (GF) and the total cell cycle time (T_c) assuming exponential growth. We present example cell count predictions obtained assuming values of GF and T_c

Table 5
Effect of uterine position on midbrain cell number

Gestational day	Slope (%)	r^2	P
11	−11	0.68	0.17
12	−7	0.62	0.01
13	−4	0.47	0.06
14	−0.8	0.03	0.65
16	0.3	0.01	0.93

The mean number of cells in each embryo was evaluated in comparison to the litter mean using linear regression. The slope indicates the percent change in cell number relative to the litter mean associated with increasing distance from the center of the uterine horn. Uterine position does appear to have a statistically significant effect on cell number on gestational day (gd) 12 ($P<0.05$) and 13 ($P<0.10$). While an overall trend of a decreasing effect of litter position with advancing age is suggested, this was not statistically significant when tested by multiple regression.

on gd 13–15 bounded by experimentally derived results on gd 12 and 16, with modifications consistent with observed changes in these parameters over the gestational period. Other combinations of values for these parameters can be assumed that also yield the observed number of cells.

Our data on changes in cell number in the developing midbrain are fairly unique. A literature search did not reveal any pre-existing data on cell number in the midbrain. For the entire embryonic CNS, Frederikson and McKay [33] reported that the total number of cells on gd 14 is approximately 1E7, or about 2.5 times the value we obtained for the midbrain on that day (4E6). Their counts were determined with dissected and dissociated brain tissue and there was likely some degree of cell loss. This appears to be the best source of comparison data in the published literature.

Our method for determining cell cycle kinetics involved administration of BrdU to label DNA in actively proliferating cells. One of the important assumptions of using the BrdU method is that BrdU itself is not affecting cell cycle kinetics. BrdU is a known teratogen in rodent species, resulting in terata such as cleft palate and decreased body weight. However, the dose of BrdU employed in studies of BrdU teratogenesis has typically been 500 mg/kg or greater, approximately 10 to 20 times that used in the current study [3–5,32]. However, a more recent study [40] reported that a dose of 120 mg/kg given to the dam during mid-gestation produced both physiological and neurobehavioral defects. On a cellular level, Boswald et al. [17] suggested that BrdU doses greater than 5 mg/kg were capable of perturbing cell kinetics in adult mouse intestinal epithelial cells. It is unclear whether this dose would also be sufficient to perturb cell kinetics in the embryonic midbrain when administered through the dam. Previous attempts we have made using BrdU doses in this range (via osmotic minipumps) did not result in sufficient labeling in the embryonic brain to allow antibody detection of cycling cells. A comparison of the cell cycle distribution between BrdU-treated animals and untreated controls in our study did not suggest any statistically significant cell cycle perturbations at a maternal dose of 25 mg/kg. The inhibitory effects of BrdU on cell cycle progression are therefore not likely to be a confounder of our results.

Conversely, if sufficient BrdU is not administered, the full fraction of cycling cells may not be detected. For example, Cameron and McKay [20] observed that doses less than 250 mg/kg failed to label all neurons in the adult dentate gyrus. They hypothesized that the blood–brain barrier impeded BrdU entry into the adult rat brain. In our case, the situation is likely to be different. The blood–brain barrier does not become fully functional in the rat until after birth and is highly permeable during the fetal period [27,70]. Thus, one might a priori expect that the level of BrdU required for labeling the embryonic rat brain would be below that required for the adult. In addition, as shown in Fig. 1, after a single pulse of 25 mg/kg, all proliferating cells were sufficiently labeled such that there were no BrdU-negative S-phase cells. Had the dose of BrdU been insufficient, either all cells would be weakly labeled (resulting in flat and shallow 'horseshoe') or the cells would be differentially labeled, resulting in a smear of S-phase cells along the *y*-axis. Neither situation was observed at gd 12 or gd 16. Thus, a dose of 25 mg/kg appeared to be sufficient to label all cells in S-phase at the time of administration. Because repeated BrdU dosing (for determination of the GF) occurred at time intervals smaller than the S-phase time, it is unlikely that some fraction of the cycling population was missed.

The data presented in this paper shed additional light on the process of development in the rodent midbrain. Our combined evaluation of changes in cell cycle kinetics and cell number appears to be fairly unique in the scientific literature. Although we studied a fairly general area of the developing brain, it should be possible, particularly at later gestational times, to apply our combined approach to more narrowly defined brain regions to help elucidate the mechanisms of specific functional deficits having a developmental origin. There has also been increasing interest in the development of biologically based models of development for evaluation of pharmaceuticals or environmental teratogens [41,69]. Data such as those collected here should be of use in the process of model development or validation and in further studies of regional variations in patterns of neuronal proliferation during development.

Acknowledgements

The authors would like to thank Julianne Hill and Martin Poot for their assistance with flow cytometric analysis of the midbrain samples. This work was supported by grants from the USEPA (grant R825358) and the jointly funded USEPA/NIEHS Child Health Center (grant R826886/ES09601).

References

[1] J. Altman, S.A. Bayer, Development of the brain stem in the rat. V. Thymidine-radiographic study of the time of origin of neurons in the midbrain tegmentum, J. Comp. Neurol. 198 (4) (1981) 677–716.

[2] J. Altman, S.A. Bayer, Atlas of Prenatal Rat Brain Development, CRC Press, Boca Raton, FL, 1995.

[3] K. Antonaides, L. Economou, A. Sioga, K. Vahtsevanos, A. Manthos, Pathogenesis of bromodeoxyuridine-induced cleft palate in mice, J. Craniomaxillofac. Surg. 23 (1995) 252–255.

[4] J. Bannigan, J. Langman, The cellular effect of 5-bromodeoxyuridine on the mammalian embryo, J. Embrol. Exp. Morph. 50 (1979) 123–135.

[5] J.G. Bannigan, The effects of 5-bromodeoxyuridine on fusion of the cranial neural folds in the mouse embryo, Teratology 32 (1985) 229–239.

[6] S.A. Bayer, J. Altman, The effects of X-irradiation on the postnatally-forming granule cell populations in the olfactory bulb,

hippocampus and cerebellum of the rat, Exp. Neurol. 48 (1975) 167–174.
[7] S.A. Bayer, J. Altman, Development of layer 1 and the subplate in the rat neocortex, Exp. Neurol. 107 (1990) 48–62.
[8] S.A. Bayer, J. Altman, Neurogenesis and neuronal migration, in: G. Paxinos (Ed.), The Rat Nervous System, 2nd Edition, Academic Press, Orlando, FL, 1995, pp. 1041–1078.
[9] S.A. Bayer, Cellular aspects of brain development, Neurotoxicology 10 (3) (1989) 307–320.
[10] S.A. Bayer, Neurogenesis in the rat primary olfactory cortex, Int. J. Neurosci. 4 (3) (1986) 251–271.
[11] S.A. Bayer, Neurogenetic patterns in the medial limbic cortex of the rat related to anatomical connections with the thalamus and striatum, Exp. Neurol. 107 (1990) 132–142.
[12] A.C. Begg, N.J. McNally, D. Shrieve, H. Karcher, A method to measure the duration of DNA synthesis and the potential doubling time from a single sample, Cytometry 6 (1985) 620–626.
[13] M. Berry, A.W. Rogers, The migration of neuroblasts in the developing cerebral cortex, J. Anat. 99 (4) (1965) 691–709.
[14] A. Bertuzzi, A. Gandolfi, C. Sinisgalli, G. Starace, P. Ubezio, Cell loss and the concept of potential doubling time, Cytometry 1;29 (1) (1997) 34–40.
[15] R. Bjugn, H.J. Gundersen, Estimate of the total number of neurons and glial and endothelial cells in the rat spinal cord by means of the optical disector, J. Comp. Neurol. 15;328 (3) (1993) 406–414.
[16] R.P. Bolender, J.S. Charleston, Software for counting cells and estimating structural volumes with the optical disector and fractionator, Microsc. Res. Tech. 25 (4) (1993) 314–324.
[17] M. Boswald, S. Harasim, B. Maurer-Schultze, Tracer dose and availability time of thymidine and bromodeoxyuridine: application of bromodeoxyuridine in cell kinetic studies, Cell. Tissue Kinet. 23 (3) (1990) 169–181.
[18] H. Braendgaard, H.J. Gundersen, The impact of recent stereological advances on quantitative studies of the nervous system, J. Neurosci. Methods 18 (1/2) (1986) 39–78.
[19] H. Braendgaard, S.M. Evans, C.V. Howard, H.J. Gundersen, The total number of neurons in the human neocortex unbiasedly estimated using optical disectors, J. Microsc. 157 (Pt 3) (1990) 285–304.
[20] H.A. Cameron, R.D. McKay, Adult neurogenesis produces a large pool of new granule cells in the dentate gyrus, J. Comp. Neurol. 435 (4) (2001) 406–417.
[21] J.S. Charleston, R.P. Bolender, N.K. Mottet, R.L. Body, M.E. Vahter, T.M. Burbacher, Increases in the number of reactive glia in the visual cortex of *Macaca fascicularis* following subclinical long-term methyl mercury exposure, Toxicol. Appl. Pharmacol. 129 (2) (1994) 196–206.
[22] J.S. Charleston, R.L. Body, R.P. Bolender, N.K. Mottet, M.E. Vahter, T.M. Burbacher, Changes in the number of astrocytes and microglia in the thalamus of the monkey *Macaca fascicularis* following long-term subclinical methylmercury exposure, Neurotoxicology 17 (1996) 127–138.
[23] J.S. Charleston, Estimating cell number in the central nervous system by stereological methods: the optical disector and fractionator, in: Current Protocols in Toxicology, Wiley, New York, 2000, pp. 1261–12619.
[24] B.H. Choi, Effects of methylmercury on neuroepithelial germinal cells in the developing telencephalic vesicles of mice, Acta Neuropathol. 81 (1991) 359–365.
[25] C. Clarke, K. Clarke, J. Muneyyirci, E. Azmitia, P.M. Whitaker-Azmitia, Prenatal cocaine delays astroglial maturation: immunodensitometry shows increased markers of immaturity (vimentin and GAP-43) and decreased proliferation and production of the growth factor S-100, Brain Res. Dev. Brain Res. 26;91 (2) (1996) 268–273.
[26] G.P. Cook, T. Chen, A.T. Koppisch, M.M. Greenberg, The effects of secondary structure and O2 on the formation of direct strand breaks upon UV irradiation of 5-bromodeoxyuridine-containing oligonucleotides, Chem. Biol. 6 (7) (1999) 451–459.
[27] E.M. Cornford, M.E. Cornford, Nutrient transport and the blood–brain barrier in developing animals, Fed. Proc. 45 (7) (1986) 2065–2072.
[28] P.N. Dean, F. Dolbeare, H. Gratzner, G.C. Rice, J.W. Gray, Cell-cycle analysis using a monoclonal antibody to BrdUrd, Cell. Tissue Kinet. 17 (4) (1984) 427–436.
[29] A. Detta, E. Hitchcock, Rapid estimation of the proliferative index of brain tumors, J. Neurooncol. 8 (1990) 245–253.
[30] F. Dolbeare, H. Gratzner, M.G. Pallavicini, J.W. Gray, Flow cytometric measurement of total DNA content and incorporated bromodeoxyuridine, Proc. Natl. Acad. Sci. USA 80 (18) (1983) 5573–5577.
[31] S.J. Duffell, A.R. Soames, S. Gunby, Morphometric analysis of the developing rat brain, Toxicol. Pathol. 28 (1) (2000) 157–163.
[32] J. Franz, J. Kleinebrecht, Teratogenic and clastogenic effects of BudR in mice, Teratology 26 (2) (1982) 195–202.
[33] K. Frederiksen, R.D.G. McKay, Proliferation and differentiation of rat neuroepithelial precursor cells in vivo, J. Neurosci. 8 (4) (1988) 1144–1151.
[34] H.J. Gundersen, P. Bagger, T.F. Bendtsen, S.M. Evans, L. Korbo, N. Marcussen, A. Moller, K. Nielsen, J.R. Nyengaard, B. Pakkenberg et al., The new stereological tools: disector, fractionator, nucleator and point sampled intercepts and their use in pathological research and diagnosis, APMIS 96 (10) (1988) 857–881.
[35] K. Hildebrandt, G. Teuchert-Noodt, R.R. Dawirs, A single neonatal dose of methamphetamine suppresses dentate granule cell proliferation in adult gerbils which is restored to control values by acute doses of haloperidol, J. Neural Transm. 106 (5/6) (1999) 549–558.
[36] J.D. Ifft, An autoradiographic study of the time of final division of neurons in rat hypothalamic nuclei, J. Comp. Neurol. 144 (2) (1972) 193–204.
[37] C. Iniguez, M.J. Gayoso, J. Carreres, A versatile and simple method for staining nervous tissue using Giemsa dye, J. Neurosci. Methods 13 (1) (1985) 77–86.
[38] K. Kharbanda, A.K. Dinda, C. Sarkar, A.K. Karak, R. Dhir, M. Mathur, S. Roy, A correlative study of in vivo and in vitro labeling index using bromodeoxyuridine in human brain tumors, J. Neurooncol. 23 (3) (1995) 185–189.
[39] T.J. Kinsella, J.B. Mitchell, A. Russo, G. Morstyn, E. Glatstein, The use of halogenated thymidine analogs as clinical radiosensitizers: rationale, current status, and future prospects: non-hypoxic cell sensitizers, Int. J. Radiat. Oncol. Biol. Phys. 10 (8) (1984) 1399–1406.
[40] B. Kolb, B. Pedersen, M. Ballermann, R. Gibb, I.Q. Whishaw, Embryonic and postnatal injections of bromodeoxyuridine produce age-dependent morphological and behavioral abnormalities, J. Neurosci. 19 (6) (1999) 2337–2346.
[41] B.G. Leroux, W.M. Leisenring, S.H. Moolgavkar, E.M. Faustman, A biologically-based dose–response model for developmental toxicology, Risk Anal. 16 (1996) 449–458.
[42] T.M. Mayhew, A review of recent advances in stereology for quantifying neural structure, J. Neurocytol. 21 (5) (1992) 313–328.
[43] T. Miki, Y. Fukui, Y. Takeuchi, M. Itoh, A quantitative study of the effects of prenatal X-irradiation on the development of cerebral cortex in rats, Neurosci. Res. 23 (3) (1995) 241–247.
[44] M.W. Miller, R.S. Nowakowski, Use of BrdU immunohistochemistry to examine the proliferation, migration and time of origin of cells in the central nervous system, Brain Res. 457 (1988) 44–52.
[45] M.W. Miller, R.S. Nowakowski, Effect of prenatal exposure to ethanol on the cell cycle kinetics and growth fraction in the proliferative zones of fetal rat cerebral cortex, Alcohol. Clin. Exp. Res. 15 (2) (1991) 229–232.
[46] M.W. Miller, Circadian rhythm of cell proliferation in the telencephalic ventricular zone: effect of in utero exposure to ethanol, Brain Res. 595 (1992) 17–24.
[47] M.W. Miller, P.E. Kuhn, Cell cycle kinetics in fetal rat cerebral cortex: effect of prenatal treatment with ethanol assessed by a

cumulative labeling technique with flow cytometry, Alcohol. Clin. Exp. Res. 19 (1995) 233–237.
[48] M.W. Miller, Limited ethanol exposure selectively alters the proliferation of precursor cells in the cerebral cortex, Alcohol. Clin. Exp. Res. 20 (1996) 139–144.
[49] D.C.P. Moore, M. Stanisstreet, G.E. Evans, Morphometric analyses of changes in cell shape in the neuroepithelium of mammalian embryos, J. Anat. 155 (1987) 87–99.
[50] R.M. Napper, J.R. West, Permanent neuronal cell loss in the cerebellum of rats exposed to continuous low blood alcohol levels during the brain growth spurt: a stereological investigation, J. Comp. Neurol. 362 (2) (1995) 283–292.
[51] R.M. Napper, J.R. West, Permanent neuronal cell loss in the inferior olive of adult rats exposed to alcohol during the brain growth spurt: a stereological investigation, Alcohol. Clin. Exp. Res. 19 (5) (1995) 1321–1326.
[52] K. Niimi, I. Harada, Y. Kusaka, S. Kishi, The ontogenetic development of the diencephalon of the mouse, Tokushima J. Exp. Med. 8 (1962) 203–238.
[53] S.C. Noctor, S.L. Palmer, T. Hasling, S.L. Juliano, Interference with the development of early generated neocortex results in disruption of radial glia and abnormal formation of neocortical layers, Cereb. Cortex 9 (2) (1999) 121–136.
[54] R.S. Nowakowski, S.B. Lewin, M.W. Miller, Bromodeoxyuridine immunohistochemical determination of the lengths of the cell cycle and the DNA-synthetic phase for an anatomically defined population, J. Neurocytol. 18 (1989) 311–318.
[55] D.E. Oorshcot, Total number of neurons in the neostriatal, pallidal, subthalamic, and substantia nigral nuclei of the rat basal ganglia: a stereological study using the cavalieri and optical disector methods, J. Comp. Neurol. 18;366 (4) (1996) 580–599.
[56] B. Pakkenberg, H.J.G. Gundersen, Total number of neurons and glial cells in human brain nuclei estimated by the disector and fractionator, J. Comp. Neurol. 384 (1997) 312–320.
[57] G. Paxinos, K.W.S. Ashwell, I. Törk, Atlas of the Developing Rat Nervous System, Academic Press, San Diego, CA, 1994.
[58] D.A. Peterson, Quantitative histology using confocal microscopy: implementation of unbiased stereology procedures, Methods 18 (4) (1999) 493–507.
[59] R.A. Ponce, T.J. Kavanagh, N.K. Mottet, S.G. Whittaker, E.M. Faustman, Effects of methyl mercury on the cell cycle of primary rat CNS cells in vitro, Toxicol. Appl. Pharmacol. 127 (1994) 83–90.
[60] T. Rasmussen, T. Schliemann, J.C. Sorensen, J. Zimmer, M.J. West, Memory impaired aged rats: no loss of principal hippocampal and subicular neurons, Neurobiol. Aging 17 (1) (1996) 143–147.
[61] M.S. Rieber, M. Rieber, UV radiation induces DNA fragmentation and cell death in B16 melanoma sensitized by bromodeoxyuridine: impaired c-jun induction and defective tyrosine phosphorylation signaling, Biochem. Biophys. Res. Commun. 203 (3) (1994) 1629–1637.
[62] P.M. Rodier, Critical periods for behavioral anomalies in mice, Environ. Health Perspect. 18 (1976) 79–83.
[63] P.M. Rodier, S.S. Reynolds, Morphological correlates of behavioral abnormalities in experimental congenital brain damage, Exp. Neurol. 57 (1) (1977) 81–93.
[64] P.M. Rodier, M. Aschner, P.R. Sager, Mitotic arrest in the developing CNS after prenatal exposure to methylmercury, Neurobehav. Toxicol. Teratol. 6 (5) (1984) 379–385.
[65] P.M. Rodier, Developing brain as a target of toxicity, Environ. Health Perspect. 103 (Suppl. 6) (1995) 73–76.
[66] C.B. Saper, Any way you cut it: a new journal policy for the use of unbiased counting methods (Editorial), J. Comp. Neurol. 364 (1996) 5.
[67] M. Shimada, T. Nakamura, Time of neuron origin in mouse hypothalamic nuclei, Exp. Neurol. 41 (1) (1973) 163–173.
[68] M. Shimada, J. Langman, Cell proliferation, migration and differentiation in the cerebral cortex of the golden hamster, J. Comp. Neurol. 139 (2) (1970) 227–244.
[69] D.L. Shuey, R.W. Setzer, C. Lau, R.M. Zucker, K.H. Elstein, M.G. Narotsky, R.J. Kavlock, J.M. Rogers, Biological modeling of 5-fluorouracil developmental toxicity, Toxicology 10 (2) (1995) 207–213.
[70] P.A. Stewart, K. Hayakawa, Early ultrastructural changes in blood–brain barrier vessels of the rat embryo, Brain Res. Dev. Res. 78 (1) (1994) 25–34.
[71] K.K. Sulik, T.W. Sadler, Postulated mechanisms underlying the development of neural tube defects. Insights from in vitro and in vivo studies, Ann. NY Acad. Sci. 15;678 (1993) 8–21.
[72] E. Taber Pierce, Histogenesis of the dorsal and ventral cochlear nuclei in the mouse. An autoradiographic study, J. Comp. Neurol. 131 (1967) 27–54.
[73] N.H.A. Terry, R.A. White, M.L. Meistrich, D.P. Calkins, Evaluation of flow cytometric methods for determining population potential doubling times using cultured cells, Cytometry 12 (1991) 234–241.
[74] N.H.A. Terry, M.L. Meistrich, R.A. White, T.A. Rich, L.J. Peters, Cell kinetic measurements as predictors of response of human tumors to radiotherapy and chemotherapy, Cancer Bull. 44 (1992) 124–129.
[75] M.J. West, H.J.G. Gunsdersen, Unbiased stereological estimation of the number of neurons in the human hippocampus, J. Comp. Neurol. 296 (1990) 1–22.
[76] M.J. West, L. Slomianka, H.J. Gundersen, Unbiased stereological estimation of the total number of neurons in the subdivisions of the rat hippocampus using the optical fractionator, Anat. Rec. 231 (4) (1991) 482–497.
[77] B.J. Wlodarczyk, G.D. Bennett, J.A. Calvin, R.H. Finnell, Arsenic-induced neural tube defects in mice: alterations in cell cycle gene expression, Reprod. Toxicol. 10 (6) (1996) 447–454.